Pure Appl. Chem., Vol. 81, No. 3, pp. 513–524, 2009.
doi:10.1351/PAC-CON-08-06-03

Gelation mechanism of ultra-high-molecular-weight polyethylene (UHMWPE) chains in dispersion solutions containing multiwall carbon nanotubes (MWNTs) analyzed in terms of liquid–liquid phase separation*

Masaru Matsuo‡, Atsuko Yamanaka, and Yumiko Nakano

Department of Textile and Apparel Science, Faculty of Human Life Environment, Nara Women's University, Nara 630-8263, Japan

Abstract: Gelation mechanisms of ultra-high-molecular-weight polyethylene (UHMWPE) in dispersion solutions containing multiwall carbon nanotubes (MWNTs) were investigated in terms of liquid–liquid phase separation mechanisms. When an incident beam of He–Ne gas laser was directed to the dispersion solution quenched to a desired temperature, the logarithm of scattered intensity increased linearly with elapsing time and tended to deviate from this linear relationship. The two different increasing behaviors of the scattered intensity were termed as initial and latter stages, respectively, of the phase separation. The linear increase in logarithmic light-scattered intensity was analyzed within the framework of the linear theory of spinodal decomposition in terms of the viewpoint that the quenched solution becomes thermodynamically unstable and tends to incur phase separation to resolve the unstable state. The growth rate of the concentration fluctuation of neat UHMWPE solution (without MWNTs) calculated from the slope of linear increase was faster than that of the dispersion solution. In spite of the rapid growth rate, however, the gelation time of the dispersion solution was much shorter than that of the neat UHMWPE solution and the gelation and quasi-spinodal temperatures were slightly higher. These phenomena were in contradiction with the result of the concentration fluctuation. This contradiction was thought to be due to the fact that diffused UHMWPE chains in the dispersion solution were gelled easily on the MWNT surface rather than the gelation by self-coagulation.

Keywords: ultra-high-molecular-weight polyethylene; multiwall carbon nanotubes; dispersion solution; liquid–liquid phase separation; spinodal decomposition.

INTRODUCTION

The gelation/crystallization method is a well-known and powerful technique to prepare ultra-high-molecular-weight polyethylene (UHMWPE), ultra-high-molecular-weight polypropylene (UHMWPP), and poly(vinyl alcohol) (PVA) films with high modulus and high strength arising from the great drawability of the resultant dry gel films. Good characteristics of UHMWPE, UHMWPP, and PVA films prepared by gelation/crystallization have led to a number of new insights for the investigation of the gela-

*Paper based on a presentation at POLYCHAR 16: World Forum on Advanced Materials, 17–21 February 2008, Lucknow, India. Other presentations are published in this issue, pp. 389–570.

‡Corresponding author: Tel./Fax: +81-742-20-3462; E-mail: m-matsuo@cc.nara-wu.ac.jp

tion mechanism. For the gelation process due to phase separation of polymer solution, there is much research that has been done by different methods, such as light-scattering [1–5], rheological [4,6], and small-angle neutron scattering (SANS) measurements [7]. The gelation mechanism has also been investigated on the basis of the time dependence of the scattered intensity of He–Ne gas laser from the gels prepared by quenching solutions.

Prins et al. firstly investigated the time dependence of scattered intensity of He–Ne gas laser to analyze the gelation mechanism of agarose when the solutions were quenched [8]. They pointed out that the initial gelation of agarose is due to the liquid–liquid phase separation associated with quasi-spinodal decomposition. Since then, more detailed analysis has been reported for several kinds of polymer. By using successful analysis of the linear theory of spinodal decomposition by Cahn [9,10], Matsuo et al. extended to some crystalline polymer solutions such as PVA [11,12], polypropylene [13], agarose [14,15], and polyethylene [16] in order to investigate whether the gelation by the quenching is attributed to the phase separation of solution by the concentration fluctuation.

Namely, the gelation mechanism of polymer solutions by quenching has been studied for PVA with intra- and intermolecular hydrogen bonds by Kanaya et al. [5] using wide- and small-angle neutron scattering and by Matsuo et al. [11,12] using X-ray diffraction, small-angle light scattering (SALS) under Hv and Vv polarization conditions, and scanning electron microscopy (SEM). Further detailed studies have been carried out by Matsuo et al. for UHMWPP [13] based on light-scattering, X-ray, infrared, and Raman measurements. Through a series of experimental results, Matsuo et al. provided conclusive evidence that when crystalline polymer solutions are quenched, the liquid–liquid phase separation associated with spinodal decomposition occurs at first and the crystallization occurs subsequently in the polymer-rich phase. Especially, phase separation of the UHMWPP solution in the gelation process was investigated in relation to the morphology and mechanical properties of the resultant dry gel film. They pointed out that the dense network structure plays an important role in assuring significant drawability in order to transmit inner stress smoothly in the stretching direction. The phase separation in the gelation process was studied by light-scattering technique to facilitate understanding of the formation of such a network structure. In spite of the detailed analysis for the UHMWPP, the time dependence of crystallite formation after rapid temperature dropping could not be measured by X-ray diffraction. For UHMWPE-quenched solution [16], it was confirmed by X-ray diffraction that there existed no ordered structure like para-crystallite with large fluctuation of lattice distance in the initial stage, but the optically anisotropic structures like rods or spherulites appeared in the later stage of the phase separation.

On the basis of a series of established results [11–16], this paper deals with the admixed effect of multiwall carbon nanotubes (MWNTs) on the gelation/crystallization mechanism of UHMWPE solutions. This is very important to make clear the evidence that well-blended UHMWPE-MWNT composites prepared by gelation/crystallization provide characteristics of high modulus and high electric conductivity. In this paper, the focus is concentrated on the time dependence of gelation in terms of the liquid–liquid phase separation of the dispersion solutions, when the dispersion solution was quenched to desired temperature. The growth rate of the concentration fluctuation of neat UHMWPE solution (without MWNTs) was faster than that of the dispersion solution. In spite of the rapid growth rate, however, the gelation time of the dispersion solution was much shorter that of the neat UHMWPE solution and also the gelation and quas-spinodal temperatures were slightly higher. These phenomena are apparently in contradiction with the result concerning the concentration fluctuation. To resolve the apparent contradiction, the detailed analysis is proposed in terms of gelation and crystallization mechanism of UHMWPE chains under the existence of MWNTs by observation of SEM.

RESULTS AND DISCUSSION

Figure 1 shows a transmission electron microscope (TEM) image and the Raman spectrum observed with an excitation laser wavelength of 488 nm of the MWNTs. The MWNTs named Hyperion Graphite

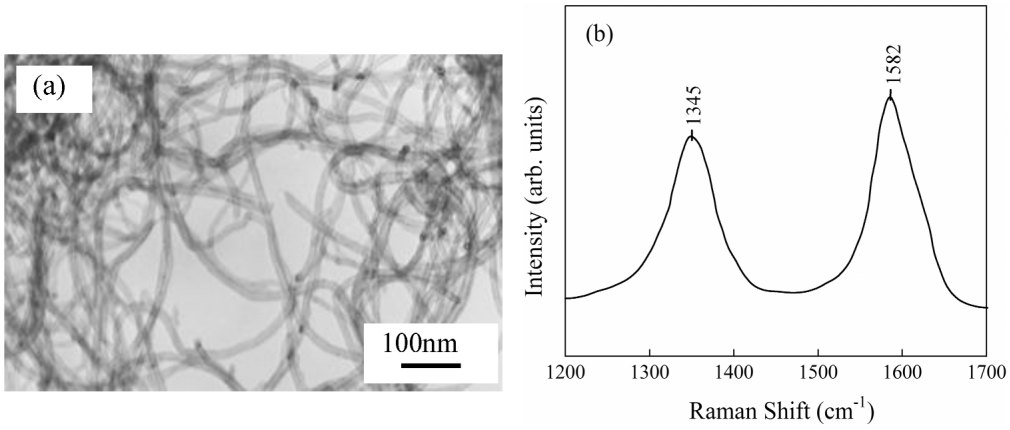

Fig. 1 (a) TEM image and (b) Raman spectrum of original MWNTs.

Fibrils were produced by Hyperion with a diameter (D) of 10–20 nm, a length (L) of 10 ~ 20 μm, and an aspect ratio (L/D) of (1 ~ 2) × 10^3. The Brunauer–Emmett–Teller (BET) surface area was 250 m^2/g, and the dibutylphthalate (DBP) adsorption was 400–500 cm^3/100 g. Image (a) indicates that the MWNTs possessed high purity and uniform diameter distribution. In Raman spectrum (b), however, the peak of the Raman-allowed phonon mode at 1582 cm^{-1} is almost the same as the intensity of the peak at 1345 cm^{-1}, which appeared through the disorder-induced phonon mode [17,18]. It indicates that the present MWNTs have a low degree of graphitization.

From preliminary experiments, as discussed before, a uniform dispersion of the present MWNTs into the UHMWPE solution could be confirmed already [20]. In preparing the homogeneous UHMWPE-MWNT dispersion solution, the contents of MWNTs were 0.015, 0.05, 0.1, 1, and 7 wt %. As for the light-scattering experiments, 0.015 wt % was the maximum concentration to detect the scattered intensity of the He–Ne gas laser (15 mW) precisely. The concentration of UHMWPE with respect to the solvent was 1 g/100 ml, because of the optimum condition to ensure a uniform dispersion of the MWNTs in solution [19]. First of all, the MWNTs in decalin solvent were treated for more than 24 h using ultrasonic treatment by batch operation, with every 20 min interval corresponding to 15 min treatment and 5 min break at ca. 25 °C. After then, UHMWPE powder was then added to the solvent containing the MWNTs, and the mixture was stirred for 30 min at 135 °C.

To determine the gelation time with respect to temperature, the test tube containing neat UHMWPE solution or UHMWPE-MWNT dispersion solution was tilted in a water bath set at constant temperature. When the meniscus deformed but the specimen did not flow under its own weight, it was judged that the solution had gelled. The interval for putting the tube in the bath was set in the time range from a few s to 3000 s. The period became longer with increasing measurable temperature.

Figure 2 shows plots of the gelation time with respect to temperature for the dispersion solutions containing 0.1 and 1 wt % MWNTs as well as for the dispersion solution containing 1 and 5 wt % carbon fiber (CF). Short CFs also used in the present experiment are MGII from Toho Tenax Co. Ltd, the average size of which was ϕ 15 × 80 μm. The length distribution is scattered from 4 to 150 μm [20]. The CFs were made from the carbonization of polyacrylonitrile (PAN). The gelation time becomes shorter with increasing MWNT and CF contents, when the dispersion solutions were quenched at the desired temperature. Especially, this tendency becomes significant, when MWNT content increases. At 80 °C, the gelation time at the dispersion solution with 1 wt % MWNT was equal to 200 s, while the gelation times of the dispersion solution with 5 wt % CF and the neat UHMWPE solution were 1400 and 2700 s, respectively. This phenomenon indicates that the dispersed MWNTs play an important role as catalyst to promote gelation/crystallization of UHMWPE chains. Accordingly, when the solution was

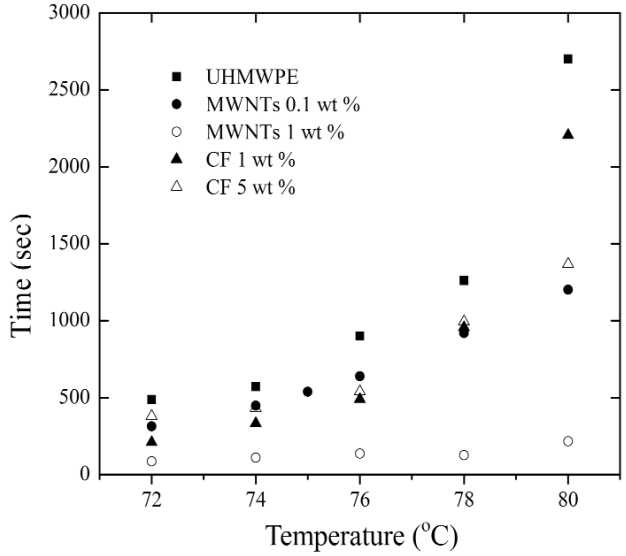

Fig. 2 Temperature dependence of gelation time of neat UHMWPE solution and the dispersion solutions containing MWNTs and CFs.

quenched, the mobility of the UHMWPE chains was less pronounced. Hence, the gelation occurred easily due to the aggregation of polymer chains, which has been known as a general concept for gel formation by cooling. Of course, cross-linking points were performed by aggregation of the UHMWPE chains, and the gel became stiffer with increasing the number of cross-linking points. The introduction of CFs promotes crystallization of the UHMWPE but this effect is not significant in comparison with the MWNTs. Accordingly, the following discussion is focused on UHMWPE-MWNT systems.

Figures 3a and b show differential scanning calorimetry (DSC) curves of the dispersion solutions containing the indicated MWNT contents under cooling and heating processes, respectively. In Fig. 3a concerning exthothermic behavior under the cooling process of the dispersion solution, it is seen that the starting of crystallization and the peak position shift to higher temperature with increasing MWNT contents. The crystallization becomes pronounced with introducing a small amount of MWNTs (0.05 wt %). Judging from the cooling speed (1 °C/min) of the DSC measurement, the crystallization temperature is thought to be close to the gelation temperature. For example, for the 1 wt % MWNT, the crystallization started at ca. 80 °C and the gelation also occurred at 200 s as can be seen in Fig. 2. The melting behavior is not sensitive to the introduction of MWNTs as shown in Fig. 3b. The melting point corresponding to the endothermic peak occurred drastically at ca. 90 °C. The endothermic curves are almost the same profile. Accordingly, the admixture of MWNTs into UHMWPE solution played an important role in promoting the gelation and crystallization of UHMWPE chains, but it was independent of the melting of crystallites in the gel.

As for the measurement of the light-scattered intensity, the dispersion solution containing the MWNTs was put in a test tube and kept at 90 °C for 5 min to avoid a drastic convection. After that, the test tube was immediately set in a time-resolved light-scattering instrument and the measurement was done at a desired temperature beyond 30 °C by using a He–Ne gas laser. The diameter of the light-scattering tube was 10 mm, and the diameter of the irradiated spots of the laser beam was set to 1 mm to ensure the construction of the ergodic hypothesis. The temperature drop was done within a few minutes [13].

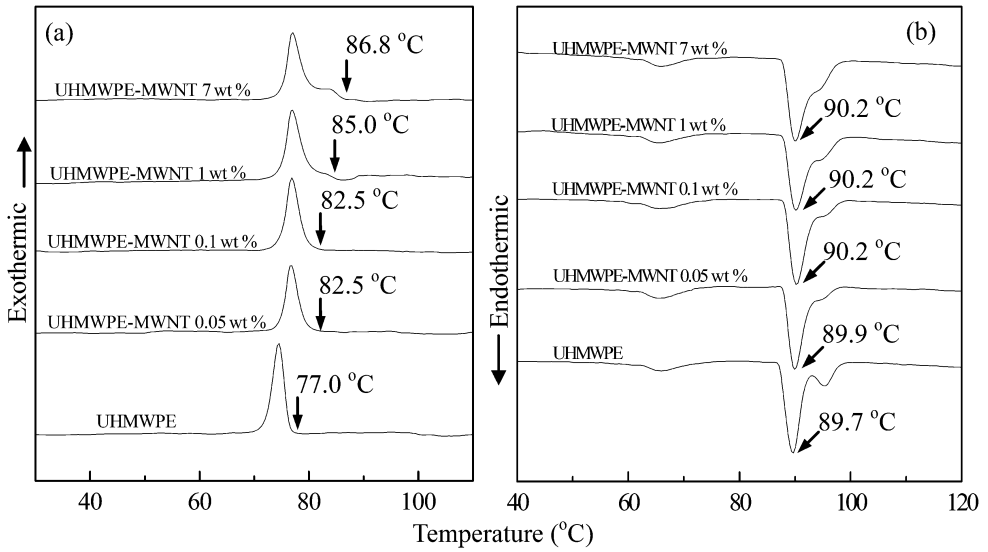

Fig. 3 DSC curves of (a) cooling process for the neat UHMWPE solution and the dispersion solution containing MWNTs with the indicated contents, and (b) heating process for the neat UHMWPE gel and the dispersion gel containing MWNTs with the indicated contents.

To check the gelation mechanism, time dependence of light-scattered intensity has been one of the effective estimations. However, the gelation of the UHMWPE solution with 1 wt % MWNT was too dark to allow investigation for the gelation mechanism by light-scattering measurements. Through trial and error, 0.015 wt % was selected as the measurable maximum content, as discussed before. The logarithm plots of the scattered intensity of He–Ne gas laser beam for the neat UHMWPE solution and the dispersion solution with 0.015 wt % MWNT were measured against time (t) at various $\boldsymbol{q}$ for the neat UHMWPE solution and the dispersion solution with 0.015 wt % MWNT, which were shown in Figs. 4 and 5, respectively. The magnitude of the scattered vector, $\boldsymbol{q}$, is given by $\boldsymbol{q} = (4\pi n/\lambda')\sin(\theta/2)$, where λ', θ, and n are the wavelength of light in solution, the scattering angle, and the refractive index of the solution, respectively.

The measurements were done in the temperature range from 65 to 80 °C. To obtain reliable results, it was necessary to check the reproducibility by the repeated experiments. The logarithm of the scattered intensity, $\ell n(I)$, increased linearly with time in the initial stage of phase separation of the solution and tended to deviate from the linear relationship. In these figures, the plots at $t = 0$ were represented as time corresponding to the beginning when the scattered intensity increased after setting the tube in the light-scattering instrument fixed at the desired temperature. The increase occurred immediately. The deviation shifted to a shorter time scale, and the slope of the linear line became steeper as the measured temperature decreased.

In accordance with the previous paper [16], the linear relationship is obviously related to the liquid–liquid phase separation of the solution. Namely, the UHMWPE solutions at elevated temperature are thermodynamically unstable at the gelation temperature and tend to incur phase separation by UHMWPE chain diffusion immediately. In such super-cooled solutions, compact molecular aggregations may be formed by chain diffusions under concentration fluctuation, and, consequently, polymer-rich phases may be formed. Under the progression of the phase separation, the aggregation of UHMWPE chains became denser with time in the polymer-rich phases.

The deviation from the linear relationship in Figs. 4 and 5 is similar to the latter stage of spinodal decomposition and successive crystallization [16]. The deviation shifts to a shorter time scale as the

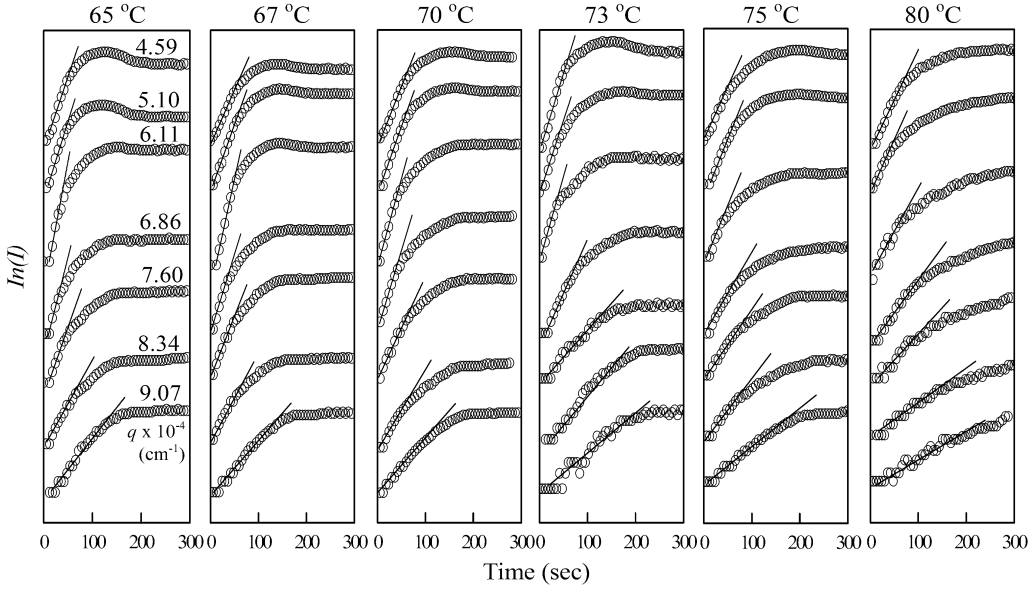

Fig. 4 Logarithm plots of the scattered intensity against time at various ***q*** observed for the 1 wt % UHMWPE solution.

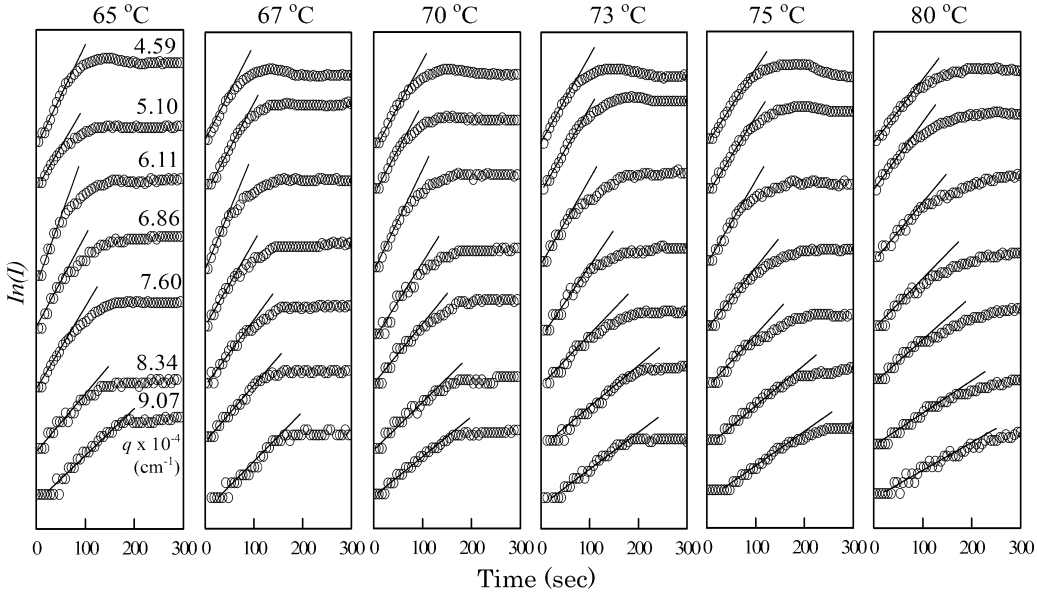

Fig. 5 Logarithm plots of the scattered intensity against time at various ***q*** observed for the dispersion solution containing 0.015 wt % MWNTs, in which the UHMWPE content is 1 wt %.

temperature decreases. Accordingly, the linear increase in $\ell n(I)$ with respect to time for the UHMWPE solutions suggests the possibility of a successful analysis of the linear theory of spinodal decomposition proposed by Cahn [9]. If the linear relationship reflects the initial stage of spinodal decomposition, as indicated by Cahn [9,10], it is well known that the change in scattered intensity in Figs. 4 and 5 can be given by

$$I(\boldsymbol{q},t) = I(\boldsymbol{q},t = 0)\exp[2R(\boldsymbol{q})t] \tag{1}$$

where $I(\boldsymbol{q},t)$ is the scattered intensity at time t, after initiation of the spinodal decomposition, and $R(\boldsymbol{q})$ is the growth rate of concentration fluctuation given as a function of $\boldsymbol{q}$, which is given by

$$R\left(\boldsymbol{q}\right) = D_{\mathrm{c}}\,\boldsymbol{q}^2\,\frac{\partial^2 f}{\partial c^2} + 2\,\kappa\boldsymbol{q}^2 \tag{2}$$

where D_{c} is the translational diffusion coefficient of the molecules in solution, f is the free energy of mixing, c is the concentration of solution, and κ is the concentration-gradient energy coefficient defined by Cahn and Hilliard [10].

In comparison with the previous results [13–16], the growth rate of concentration fluctuation $R(\boldsymbol{q})$ for neat UHMWPE solution became higher, as the concentration increased. This means that $R(\boldsymbol{q})$ is not closely related to viscosity of the solution but is associated with the coagulation speed of UHMWPE chains to form gels. Accordingly, the period of the initial stage becomes shorter with increasing the concentration, and, consequently, the formations of network structures and crystallization occur rapidly. However, if this is the case, the slope of the dispersion solution must be steeper than that of the neat UHMWPE solution. To check it, the values of $R(\boldsymbol{q})$ are plotted against $\boldsymbol{q}$.

Figure 6 shows the growth rate of concentration fluctuation $R(\boldsymbol{q})$ plotted against $\boldsymbol{q}$ for the UHMWPE solution and the dispersion solution. The maximum growth rate $R(\boldsymbol{q}_{\mathrm{max}})$ increased with decreasing measured temperature T and the value of the corresponding scattering vector, $\boldsymbol{q}_m$, was maintained at the same angle. This phenomenon is in good agreement with the principle of spinodal decomposition for the amorphous polymer solutions proposed by van Aartsen [21], if the spinodal temperature T_{s} is higher than 80 °C. The growth of the concentration fluctuation in the initial stage promotes the molecular aggregation and crystallization in the later stage. However, the spinodal ring did not appear because of the dull scattering maximum. To observe it, the peak must usually be 2 or 3 orders of magnitude greater. Judging from the curves in Figs. 6a and b, the fluctuation of UHMWPE chains in the neat solution is thought to be more considerable than that in the dispersion solution. This apparently contradicts the fact that the gelation time of the dispersion solution is shorter than that of the neat solution in Fig. 2. This essential interesting phenomenon shall be discussed later.

To give more conclusive evidence for spinodal decomposition based on the linear relationship, the spinodal temperature T_{s} was estimated according to the linear theory. To do so, plots of $R(\boldsymbol{q})/\boldsymbol{q}^2$ vs. $\boldsymbol{q}^2$ were performed at the measured temperature. The plots showed a linear relationship and the apparent diffusion coefficient D_{app}, defined by $D_{\mathrm{app}} = D_{\mathrm{c}}(\partial^2 f/\partial c^2)$, can be obtained by the intercept on the vertical axis. Here, it should be noted that the values of $D_{\mathrm{app}} = -D_{\mathrm{c}}(\partial^2 f/\partial c^2)$ are significant. Due to the positive values of D_{c} by definition, the values of $\partial^2 f/\partial c^2$ took a negative value characterizing unstable regions, leading to spinodal decomposition.

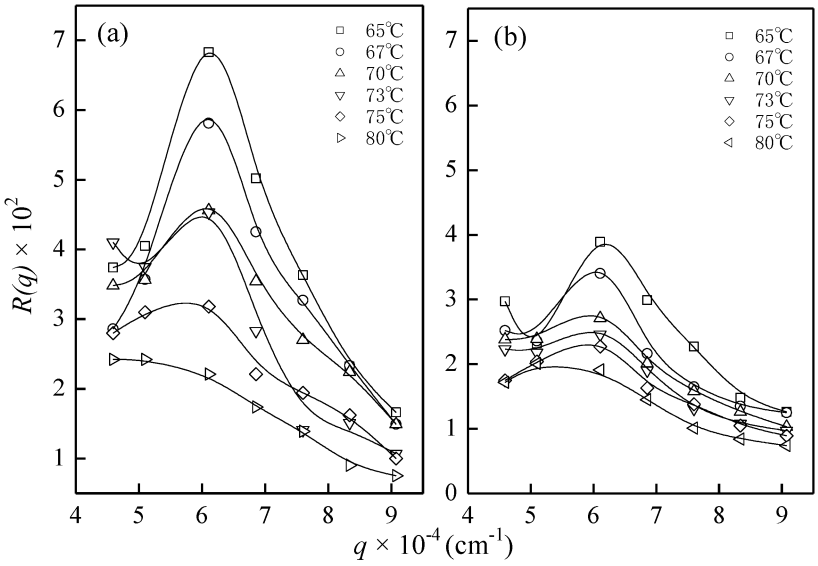

Fig. 6 Growth rate of concentration fluctuation $R(\boldsymbol{q})$ against $\boldsymbol{q}$ estimated for (a) 1 wt % UHMWPE solution and (b) the dispersion solution containing 0.015 wt % MWNT.

Figures 7a and b show the temperature dependence of D_{app} for the neat UHMWPE solution and the dispersion solution, respectively. A fairly good linear relationship was also obtained. From the intercept on the temperature axis, one can define the spinodal temperature T_s at $D_{app} = 0$. T_s of the UHMWPE-MWNT dispersion solution was slightly higher than that of the neat UHMWPE solution. The higher T_s of the dispersion solution is in good agreement with higher gelation temperature in comparison with the neat solution. This indicates that UHMWPE chains afforded by admixing a small amount of MWNTs, incurred rapid formation of cross-linking points to accelerate gelation in spite of a slow growth rate of concentration fluctuation at 65 ~ 80 °C.

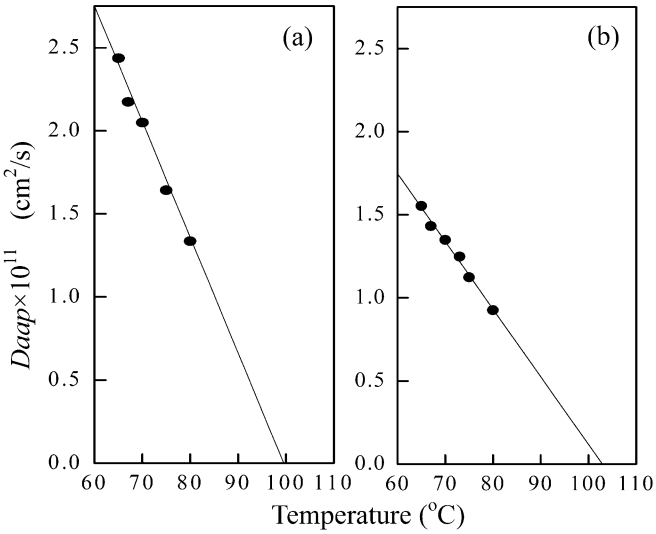

Fig. 7 Temperature dependence of D_{app} for the 1 wt % UHMWPE solution and the dispersion solution containing 0.015 wt % MWNT.

Here it is of interest to consider whether the spinodal temperature (T_s) is useful for understanding the detailed gelation mechanism. Although T_s was determined in the initial stage of spinodal decomposition shorter than 200 s, it was confirmed that any optical anisotropic structure associated with gelation beyond 3 h did not appear at 100 °C for neat solution and at 105 °C for the dispersion solution.

As shown in Fig. 8, for example, the polarizing optical microscopy (POM) photograph of UHMWPE solution quenched at 98 °C close to T_s (= 99.5 °C) showed no superstructure, but the superstructure could be observed after 30 min when the solution was quenched at 93 °C lower than T_s. On the other hand, the image of the dispersion solution quenched at 98 °C lower than T_s (102.9 °C) showed superstructures after 30 min.

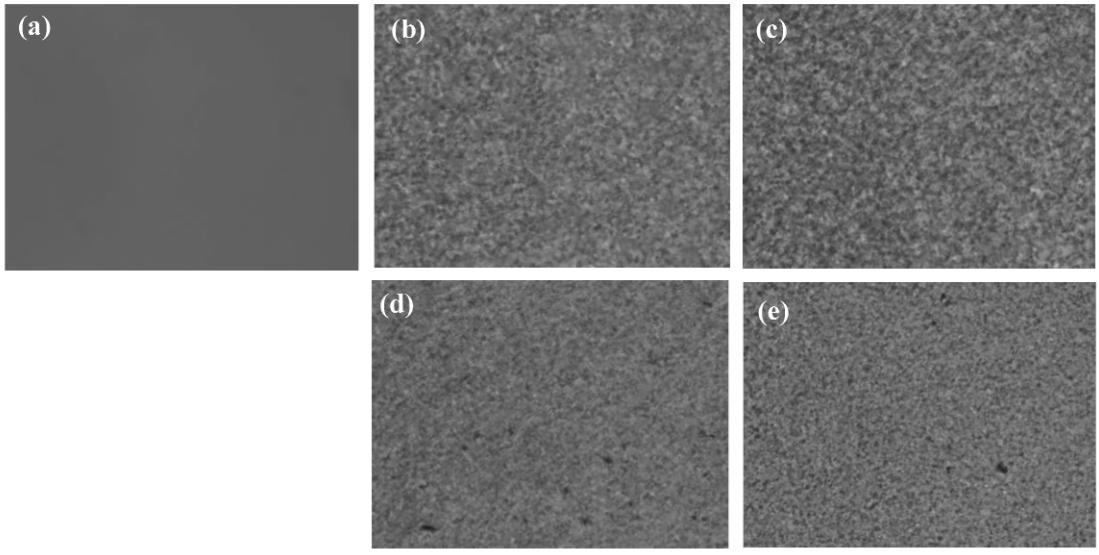

Fig. 8 Polarized micrographs of the UHMWPE solution and the dispersion solution at the indicated temperatures. UHMWPE solution (a) at 3 h after quenching at 98 °C, (b) at 30 min after quenching at 93 °C, (c) at 2 h after quenching at 93 °C, (d) the dispersion solution at 30 min after quenching at 98 °C, (e) at 1 h after quenching 98 °C.

Figure 9 shows the small-angle light-scattering patterns under polarized condition termed as Hv scattering. The patterns were observed from the neat solution and the dispersion solutions quenched at the indicated temperature. For example, the 70 °C – 6 min means the pattern from the neat UHMWPE solution maintained for 6 min after quenching it at 70 °C. It was confirmed that the patterns were not observed from the neat and dispersion solutions in the period assuring linear plots of $\ell n(I)$ against time in Figs. 4 and 5. This indicates that the Hv scattering did not appear in the initial stage of the phase separation but appeared at the later stage.

An indistinct Hv scattering pattern with the X-type lobes could be observed in the later stage at temperatures lower than T_s, and the corresponding polarized microscopy provided indistinct non-color superstructures. The Hv scattering mode is different from the mode under the gelation process of agarose [14,15], and PVA [11] with a perfectly dark POM photograph. In comparison with the POM photos in Fig. 8, the Hv pattern from gels prepared at temperatures $<T_s$ are attributed to scattering from rod-like structures with very large disordered UHMWPE chains, while the diffuse scattering from the neat solution at 98 °C and the dispersion solution at 103 °C are due to scattering from optical elements with large correlation distance.

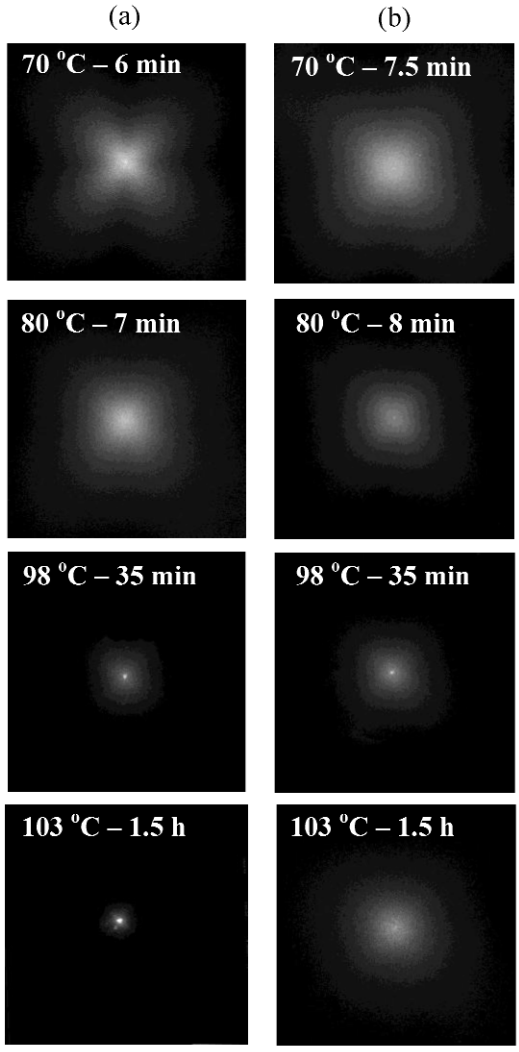

Fig. 9 Hv light-scattering patterns from (a) the UHMWPE and (b) the dispersion solutions taken at the indicated time after quenching at the indicated temperatures.

Here we shall discuss the contradiction discussed above. That is, as shown in Figs. 2 and 7, the gelation time of the dispersion solution is much shorter than that of the neat solution in spite of slow growth rate of the concentration fluctuation. This contradiction is due to the different gelation mechanisms between the neat and dispersion solutions. As the general concept, when the solution was quenched, the quenched solution becomes thermodynamically unstable and tends to incur phase separation to resolve the unstable state by the concentration fluctuation. The gelation time becomes shorter, as the growth rate of the concentration fluctuation is faster. If this is the case, the gelation time of the neat solution must be shorter than that of the dispersion solution with MWNTs. However, the experimental result is in a reverse order as shown in Fig. 2. This is due to the fact that the gelation/crystallization of UHMWPE chains in the dispersion solution occurred on the surface of the MWNTs. Then, the diffusion of UHMWPE chain occurred to resolve the unstable state. The diffusion chains come into collision with MWNTs with network structure, and the gelation of the UHMWPE chains occurred on the surface easily. It may be expected that the possibility was very high, and, consequently, the gelation

of UHMWPE chains in the dispersed solution occurred on the surface of MWNTs before performing polymer-rich phase by self-coagulation of the chains. The gelation on the MWNT surface formed cross-linked networks of UHMWPE chains and crystallization of the cross-linking points occurred. This mechanism could be demonstrated by SEM images of the dried gel composites.

Figures 10a and b show the cross-section area of the composites after evaporating solvent, in which (a) and (b) are images of the composites before and after heat-treatment at ca. 150 °C [22]. In comparison with the original MWNTs in Fig. 1a, it is seen that the MWNTs within the original composite before the heat treatment were covered by UHMWPE and their average diameter was much thicker than that of the original MWNTs. This indicated that the most of UHMWPE chains were gelled and crystallized on the MWNTs. In contrast, image (b) reveals that the average diameter of the composite after the heat treatment showed a similar size to that of the original MWNTs as shown in Fig. 1a. Namely, overlapped bare MWNTs were dispersed with UHMWPE matrix. This means that most of the melted UHMWPE chains were removed from the MWNT surfaces, and recrystallization of UHMWPE chains under the cooling process did not occur on the MWNT surface. Actually, this phenomenon provided a drastic increase in electric conductivity of the composite after the heat treatment, since electron transfer by the direct contact between adjacent MWNTs became more active in comparison with the electron transfer between adjacent MWNTs covered by UHMWPE [2,22].

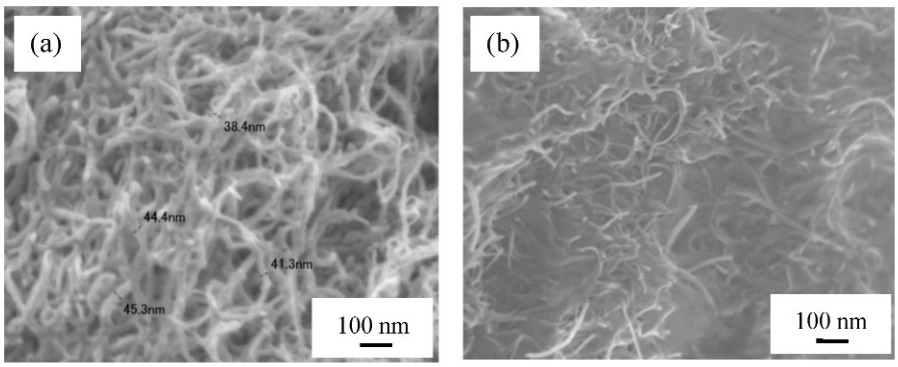

Fig. 10 SEM images of the cross-section area of (a) original dry gel film and (b) the gel annealed at 150 °C.

CONCLUSION

To investigate well-mixed composite of UHMWPE and MWBNTs, gelation mechanisms of UHMWPE chains in dispersion solutions containing MWNTs were investigated by using He–Ne gas laser, DSC, SEM, and POM. The gels were prepared by quenching the dispersion solutions with different MWNT contents, and the mechanism was analyzed in terms of the concentration fluctuation. When an incident beam of He–Ne gas laser was directed to the dispersion solution quenched to a desired temperature, the logarithm of scattered intensity increased linearly with elapsing time and tended to deviate from this linear relationship. The two different increasing behaviors of the scattered intensity were termed as initial and latter stages, respectively, of the phase separation due to quasi-spinodal decomposition. Above the quasi-spinodal temperature (T_s) estimated by the linear theory of Cahn, the gelation occurred indicating that the concentration fluctuation of UHMWPE chains played an important role in promoting the gelation. The growth rate of the concentration fluctuation of neat UHMWPE solution (without MWNTs) was faster than that of the dispersion solution. In spite of the rapid growth rate, the gelation time of the dispersion solution was much shorter that of the neat UHMWPE solution. Such contradiction was analyzed by SEM observation of the dry gel film prepared after evaporating solvent. Per the observation, it was seen that the average diameter of the MWNTs in the film was much thicker than that

of the original MWNTs. This indicated that most UHMWPE chains were gelled and crystallized on the MWNTs. This indicated that the diffusion UHMWPE chains came into collision with MWNTs with network structure and the gelation of the UHMWPE chains occurred on the surface easily. Accordingly, it turned out that the gelation of UHMWPE chains in the dispersed solution occurred on the surface of MWNTs before performing polymer-rich phase by self-coagulation of the chains, and then the gelation on the MWNT surface promoted the formation of cross-linked networks and crystallization of the cross-linking points occurred.

REFERENCES

1. M. Tsujimoto, M. Shibayama. *Macromolecules* **35**, 1342 (2002).
2. H. Takeshita, T. Kanaya, K. Nishida, K. Kaji. *Macromolecules* **32**, 7815 (1999).
3. A. L. Kjoniksen, B. Nystrom. *Macromolecules* **29**, 7116 (1996).
4. B. Wang, S. Mukataka, M. Kodama, E. Kokufuta. *Langmuir* **13**, 6108 (1997).
5. T. Kanaya, M. Ohkura, K. Kaji, M. Furusaka, M. Misawa. *Macromolecules* **27**, 5609 (1993).
6. J. H. Chio, S. W. Ko, J. Blackwell, W. S. Lyoo. *Macromolecules* **34**, 2964 (2001).
7. F. Auriemma, C. D. Rosa, R. Triolo. *Macromolecules* **39**, 9429 (2006).
8. E. Pines, W. Prins. *Macromolecules* **6**, 888 (1973).
9. J. W. Cahn. *J. Chem. Phys.* **42**, 93 (1965).
10. J. W. Cahn, J. E. Hilliard. *J. Chem. Phys*. **28**, 258 (1958).
11. M. Matsuo, K. Kawase, Y. Sugiura, S. Takematsu, C. Hara. *Macromolecules* **26**, 4461 (1993).
12. M. Matsuo, Y. Sugiura, S. Takematssu, T. Ogita, T. Sakabe, R. Nakamura. *Polymer* **38**, 5953 (1997).
13. M. Matsuo, T. Hashida, K. Tashiro, Y. Agari. *Macromolecules* **35**, 3030 (2002).
14. M. Matsuo, T. Tanaka, L. Ma. *Polymer* **43**, 5299 (2002).
15. M. Matsuo, S. Miyoshi, M. Azuma, Y. Nakano, Y. Bin. *Phys. Rev. E* **72**, 041403 (2005).
16. M. Matsuo, S. Miyoshi, A. Azuma, Y. Bin, Y. Agari, Y. Satoh, A. Kondo. *Macromolecules* **38**, 6688 (2005).
17. R. J. Nemanish, S. A. Solin. *Phys. Rev. B* **20**, 392 (1979).
18. C. P. An, Z. V. Vardeny, Z. Iqbal, G. Spinks, R. H. Baughman, A. Zakhidov. *Synth. Met.* **116**, 411 (2001).
19. Y. Bin, M. Kitanaka, D. Zhu, M. Matsuo. *Macromolecules* **36**, 6213 (2003).
20. Y. Xi, H. Ishikawa, Y. Bin, M. Matsuo. *Carbon* **42**, 1699 (2004).
21. J. J.van Aartsen. *Eur. Polym. J.* **6**, 919 (1970).
22. Y. Bin, A. Yamanaka, Q. Chen, Y. Xi, X. Jiang, M. Matsuo. *Polym. J.* **39**, 598 (2007).
23. Q. Chen, Y. Bin, M. Matsuo. *Macromolecules* **39**, 6528 (2006).